Discovery of a Novel Class of Potent Human Deoxyuridine Triphosphatase Inhibitors Remarkably Enhancing the Antitumor Activity of Thymidylate Synthase Inhibitors

Seiji Miyahara,[†,‡] Hitoshi Miyakoshi,[†,§] Tatsushi Yokogawa,[†] Khoon Tee Chong,[†] Junko Taguchi,[†] Toshiharu Muto,[†] Kanji Endoh,[†] Wakako Yano,[†] Takeshi Wakasa,[†] Hiroyuki Ueno,[†] Yayoi Takao,[†] Akio, Fujioka,[†] Akihiro Hashimoto,[†] Kenjirou Itou,[†] Keisuke Yamamura,[†] Makoto Nomura,[†] Hideko Nagasawa,[§] Satoshi Shuto,[‡] and Masayoshi Fukuoka*,[†]

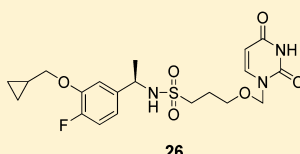[†]Tsukuba Research Center, Taiho Pharmaceutical Co. Ltd., Okubo 3, Tsukuba, Ibaraki 300-2611, Japan
[‡]Faculty of Pharmaceutical Sciences, Hokkaido University, Kita-12, Nishi-6, Kita-ku, Sapporo 060-0812, Japan
[§]Laboratory of Pharmaceutical and Medicinal Chemistry, Gifu Pharmaceutical University, 1-25-4 Daigaku-nishi, Gifu 501-1196, Japan
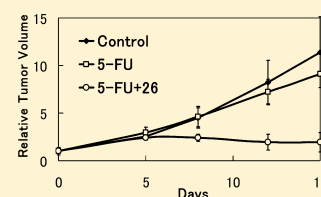
Ⓢ *Supporting Information*

ABSTRACT: Inhibition of human deoxyuridine triphosphatase (dUTPase) has been identified as a promising approach to enhance the efficacy of 5-fluorouracil (5-FU)-based chemotherapy. This study describes the development of a novel class of dUTPase inhibitors based on the structure–activity relationship (SAR) studies of uracil derivatives. Starting from the weak inhibitor **7** (IC_{50} = 100 μM), we developed compound **26**, which is the most potent human dUTPase inhibitor (IC_{50} = 0.021 μM) reported to date. Not only does

A novel human dUTPase inhibitor

26
human dUTPase IC_{50} = 21 nM

compound **26** significantly enhance the growth inhibition activity of 5-fluoro-2′-deoxyuridine (FdUrd) against HeLa S3 cells in vitro (EC_{50} = 0.075 μM) but also shows robust antitumor activity against MX-1 breast cancer xenograft model in mice when administered orally with a continuous infusion of 5-FU. This is the first in vivo evidence that human dUTPase inhibitors enhance the antitumor activity of TS inhibitors. On the basis of these findings, it was concluded that compound **26** is a promising candidate for clinical development.

INTRODUCTION

Thymidylate synthase (TS) inhibitors including 5-fluorouracil (5-FU) and its derivatives are widely used in clinical cancer chemotherapy.[1−4] Although TS inhibitors are significantly beneficial, a large percentage of tumors exhibit intrinsic or acquired drug resistance.[5] Therefore, novel therapeutic targets and strategies are urgently required to overcome the frequent occurrence of drug resistance.

TS inhibitors lead to rapid depletion of the cellular 2′-deoxyuridine 5′-triphosphate (dTTP) pool. Depletion of dTTP pool induces thymineless death. In addition, TS inhibition results in the accumulation of 2′-deoxyuridine 5′-monophosphate (dUMP), which may subsequently lead to increased levels of 2′-deoxyuridine 5′-triphosphate (dUTP).[6,7] Both dUTP and the 5-FU metabolite 5-fluoro-2′-deoxyuridine 5′-triphosphate (FdUTP) can be misincorpotated into DNA in place of dTTP during replication and repair by DNA polymerase.[8] High cellular (F)dUTP/dTTP ratios induce futile cycles of misincorporation; these cycles eventually lead to DNA strand breaks and cell death. This is one of the key antitumor mechanisms of TS inhibitors.[9−13]

dUTPase is a preventive DNA repair enzyme with exquisite specificity for dUTP among canonical nucleoside triphosphates; it hydrolyzes dUTP to dUMP and inorganic pyrophosphate.[14−16] This enzyme serves two functions in nucleotide metabolism: first, it decreases the amount of intracellular dUTP pools to prevent the misincorporation of uracil instead of thymine into DNA, and second, it supplies the substrate dUMP for TS, which is responsible for an important de novo nucleotide metabolism pathway in DNA synthesis.[17] In addition, it has been reported that dUTPase can hydrolyze FdUTP.[18] Accordingly, increased dUTPase activity induces resistance to TS inhibitors. Basic research on the relationship between the sensitivity of TS inhibitors and expression of dUTPase has been reported previously. Elevation of dUTPase activity correlates with resistance to FdUrd in colorectal and breast cancer cell lines,[19−21] and small interfering RNA-mediated suppression of human dUTPase enhances the growth inhibition activity of FdUrd against SW620 and MCF-7 cells by expansion of the dUTP pool in vitro.[12]

On the basis of the analysis of human tissue specimens, Ladner and co-workers reported that nuclear dUTPase overexpression may correlate with resistance to TS inhibitor-

based cancer chemotherapy and poor prognosis in colorectal cancer.[22] Furthermore, Takatori and co-workers have reported that nuclear dUTPase activation significantly correlates with poor survival outcomes in patients with hepatocellular carcinoma (HCC).[23] These findings demonstrate that human dUTPase inhibitors could be clinically useful agents that enhance the antitumor activity of TS inhibitors.

Thus, efforts to obtain efficient dUTPase inhibitors have resulted in the development of several compounds (Figure 1).
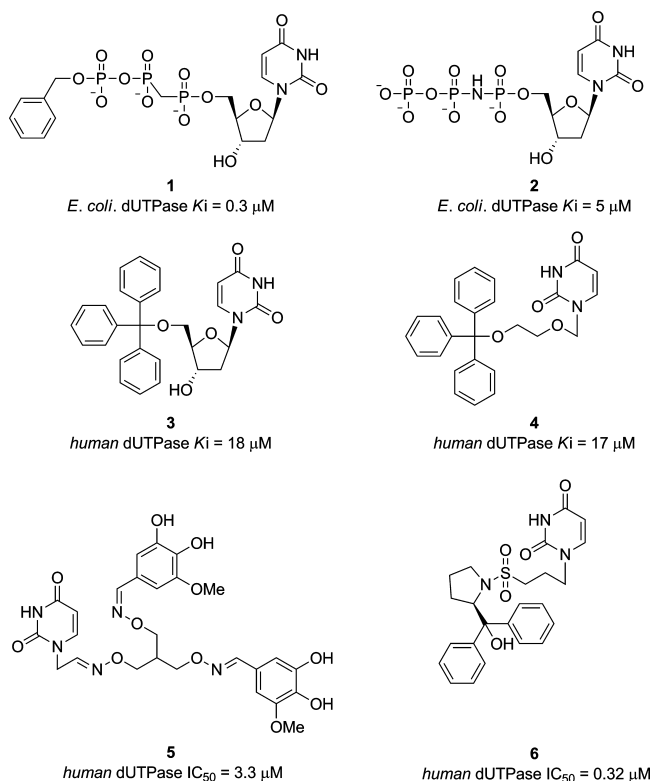
Figure 1. Chemical structures of BM-dUTP **1**,[24] dUPNPP **2**,[25] 5′-O-trityl-2′-deoxyuridine **3**,[29] acyclouridine derivative **4**,[31] oxime-linkage compound **5**,[33] and our previous inhibitor **6**.[34]

For example, nonhydrolyzable isosteres **1** and **2** of the substrate dUTP have been synthesized in which the oxygen atom between the α- and β-phosphates of the triphosphate moiety of dUTP is replaced by a methylene or an imino group.[24,25] These compounds had a low K_i value against *Escherichia coli* dUTPase and were effectively used in kinetic studies[26,27] and for solving the X-ray crystal structures of the enzyme from various species.[28] However, these nonhydrolyzable inhibitors appear to be ineffective for chemotherapeutic uses owing to high polarity and consequent poor cell membrane permeability. In addition, enzyme inhibitors without a phosphate or its isostere such as 5′-O-substituted deoxyuridine derivatives **3**[29,30] and acyclouridine derivatives **4**[31,32] have been reported. Although these compounds have inhibition activity against the dUTPase of *Plasmodium faliciparum*, their inhibition activity against human dUTPase is weak. Stivers and co-workers have synthesized oxime-linkage compounds such as **5**[33] that only moderately inhibited human dUTPase.

In our previous paper, we reported the discovery of N-1 substituted uracil derivatives, such as compound **6**, as dUTPase inhibitor with a unique binding mode and potent enzyme inhibition activity (IC$_{50}$ values in the 10^{-7} M range in vitro).[34]

In this report, we describe the discovery of a novel class of dUTPase inhibitors with increased inhibition activity (IC$_{50}$ values in the 10^{-8} M range). Furthermore, we found that compound **26** is the first human dUTPase inhibitor that remarkably enhances the antitumor activity of a TS inhibitor in vivo. Our present study provides compelling evidence that the small molecule dUTPase inhibitor may provide a promising novel cancer therapeutic strategy.

RESULT AND DISCUSSION

Identification of an Initial Lead Compound 9. Human dUTPase has an exquisite substrate specificity only for dUTP among the canonical nucleoside triphosphates. Thus, human trimeric dUTPase specifically recognizes a uracil ring in the active site pockets located at the three subunit interfaces of the dUTPase trimer.[35,36] On the basis of this fact, we prepared our own N-1 substituted uracil derivatives library and examined the enzyme inhibition activity of constituent compounds to identify novel scaffolds (hit compounds) that could be used for designing potent human dUTPase inhibitors. Throughout this study, we found several classes of weak dUTPase inhibitors. Among these compounds, we focused our attention on 1-((2-(*tert*-butyldimethylsilyloxy)ethoxy)methyl)pyrimidine-2,4-(1*H*,3*H*)-dione **7** (IC$_{50}$ = 100 μM) as a prototype compound that could be used to develop efficient inhibitors because of its low molecular weight and amenability to derivatization.

Substructure searches of compound **7** led to the identification of compound **8** and **9** that have still low molecular weight and enable further structural modification (Figure 2). In enzyme inhibition assays, these compounds
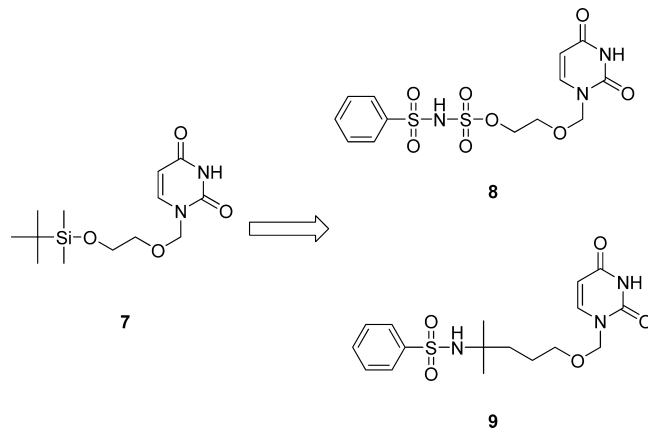
**Figure 2.** Structures of compound **7**, **8**, and **9**.

exhibited increased dUTPase inhibition activity (IC$_{50}$ = 3.1, 3.9 μM) compared with those of the hit compound **7** and the previously reported inhibitors **2** and **4** (Table 1).

To investigate whether compounds **8** and **9** enhance the cell growth inhibition activity of FdUrd, we performed a growth inhibition assay in combination with FdUrd in HeLa S3 cells. The EC$_{50}$ value represents the concentration of each compound that reduces the T/C (%) value of FdUrd (1 μM) against HeLa S3 cells to half in 24 h. Compound **8** did not enhance the growth inhibition activity of FdUrd in vitro. The acidity of compound **8** may have led to the lack of cell membrane permeability. On the other hand, compound **9** clearly enhanced the growth inhibition activity of FdUrd (1 μM) in a concentration dependent manner (EC$_{50}$ = 5.1 μM) in vitro (Figure 3). Treatment with **9** alone had little effect on cell

Table 1. Enzyme Inhibition Activities of Human dUTPase Inhibitors

compd	IC$_{50}$ (μM)^a
2	15.2 ± 1.4
4	>100
7	100
8	3.1 ± 0.30
9	3.9 ± 0.63

^{a}Concentration of each compound required to inhibit 50% of the amount of [5-^{3}H]dUMP produced by human dUTPase. IC$_{50}$ data represent the average of three independent assays unless otherwise stated. Errors are given as standard deviations.
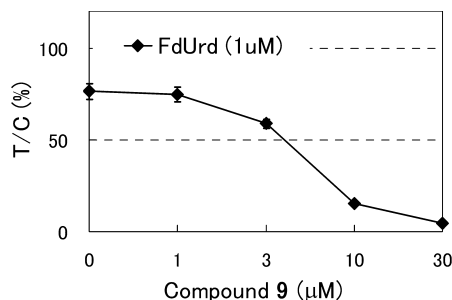
Figure 3. Enhancing effect of compound **9** for growth inhibition activity of FdUrd (1 μM) against HeLa S3 cells.

growth (T/C 96% at 30 μM). These results suggest that compound **9** enhanced the growth inhibition activity of FdUrd by inhibiting human dUTPase in HeLa S3 cells.

To elucidate the binding mode of compound **9** to human dUTPase, an X-ray crystal structure of the trimeric human dUTPase complexed with compound **9** was solved at 1.8 Å resolution. This clearly demonstrated the defined binding mode in which compound **9** is accommodated in the active site located at the three subunit interfaces between each subunit of the dUTPase trimer. Some interactions of compound **9** with the enzyme in the active site were observed as shown in Figure 4A. Uracil O4 form two hydrogen bonds with the amide NH group of Val 112 and the carbonyl group of Gly97 via a water molecule, and it forms another hydrogen bond with the amide NH group of Gly99. Uracil N-3 interacts with the carbonyl group of Gly110, and uracil O2 forms a hydrogen bond with

the amide NH group of Gly110. The sulfonamide NH group of compound **9** interacts with the hydroxyl group of Tyr105 via two water molecules. In Figure 4B, compound **9** was superimposed on the X-ray cocrystal structure of dUPNPP **2** with human dUTPase. Compound **9** adopts a folded conformation in the active site of the enzyme that is similar to **6**, as reported in our previous paper.[34] The uracil ring of compound **9** is accommodated in the conserved uracil binding site, and its terminal phenyl ring is located in the relatively hydrophobic region (formed by Val65, Ala90, Ala98, and Val112) of the enzyme.

The C-terminal residues of each subunit of dUTPase, which are invariably disordered in the uncomplexed structure (open form), become ordered upon dUTP binding to each of the active sites (closed form) (Figure 5).[35,36] It may be crucial for the enzymatic activity of human dUTPase that the flexible C-terminal tail locates to each ligand binding active site, where the uracil ring of the substrate and the phenyl group of Phe158 in the enzyme are stacked. The terminal phenyl ring of compound **6** prevented the alignment of the flexible phenyl group of Phe158 to the active site without any interaction between the inhibitor and the triphosphate-binding pocket.[34] X-ray cocrystal structures show that compound **9** binds in a similar manner to compound **6**, with the terminal phenyl ring occupying a region similar to that of Phe158. Therefore, the C-terminal tail that includes Phe158 cannot be detected in the active site.

Improvement of the Initial Lead Compound 9. Part 1: Substitution at the Phenyl Ring. We next investigated the substituent effects at the terminal phenyl ring of compound **9**. A series of analogues **9** (**10**−**16**) were synthesized starting from commercially available compound **17** (Scheme 1). Reduction of nitro and ester groups of compound **17** with lithium aluminum hydride (LiAlH$_4$) followed by treatment with *N*-carbobenzoxyoxysuccinimide afforded **18**, which was further treated with chloromethyl methyl ether (MOMCl) to afford **19**. After activation of the methoxymethyl (MOM) group of **19** by boron trichloride (BCl$_3$), treatment with 2,4-bis(trimethylsilyloxy)-pyrimidine {(TMS)$_2$uracil} afforded **20**. Removal of the carbobenzyloxy group and subsequent sulfonylation afforded **9**−**15**. Compound **16** was synthesized from intermediate **19** by removal of the carbobenzyloxy group, sulfonylation of the primary amine, benzoyl group deprotection by methylamine,
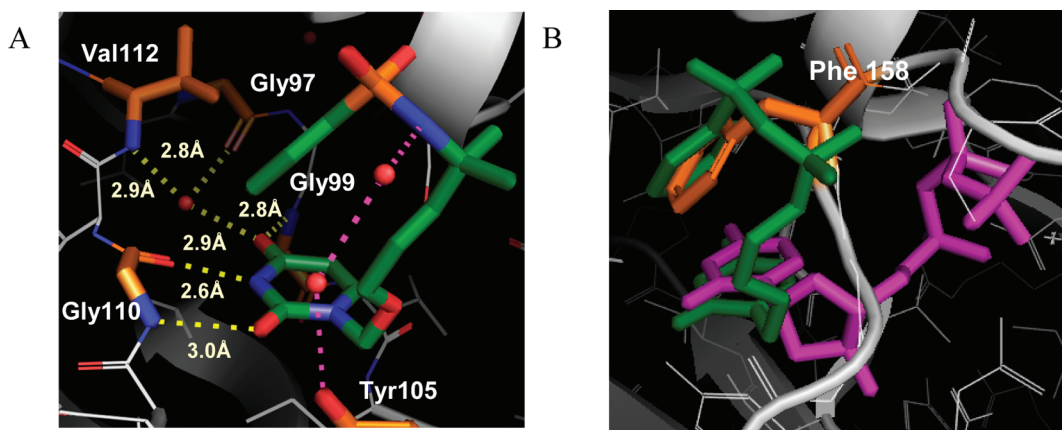
Figure 4. (A) X-ray cocrystal structure of compound **9** (green) with human dUTPase (PDB code: 3ARN). Water molecules are shown as small spheres. Compound **9** forms key hydrogen bond contacts (yellow dotted lines) with the enzyme. (B) Overlay of compound **9** and X-ray cocrystal structure of dUPNPP **2** (magenta) with human dUTPase (PDB code: 2HQU). Phe158 is highlighted in orange.
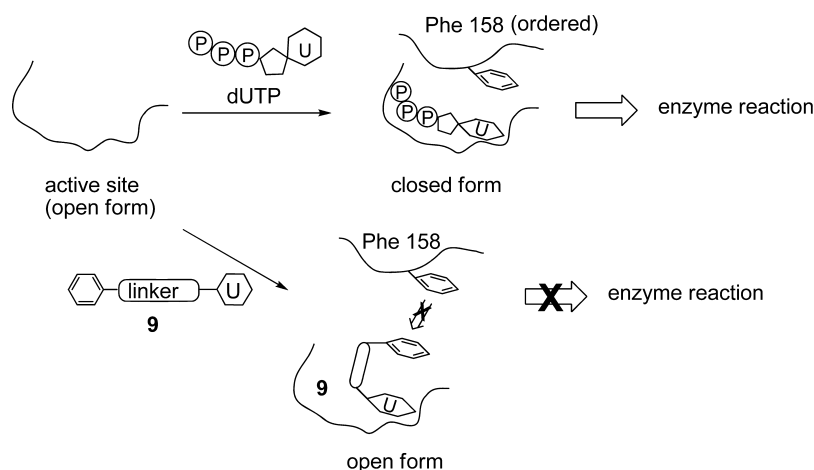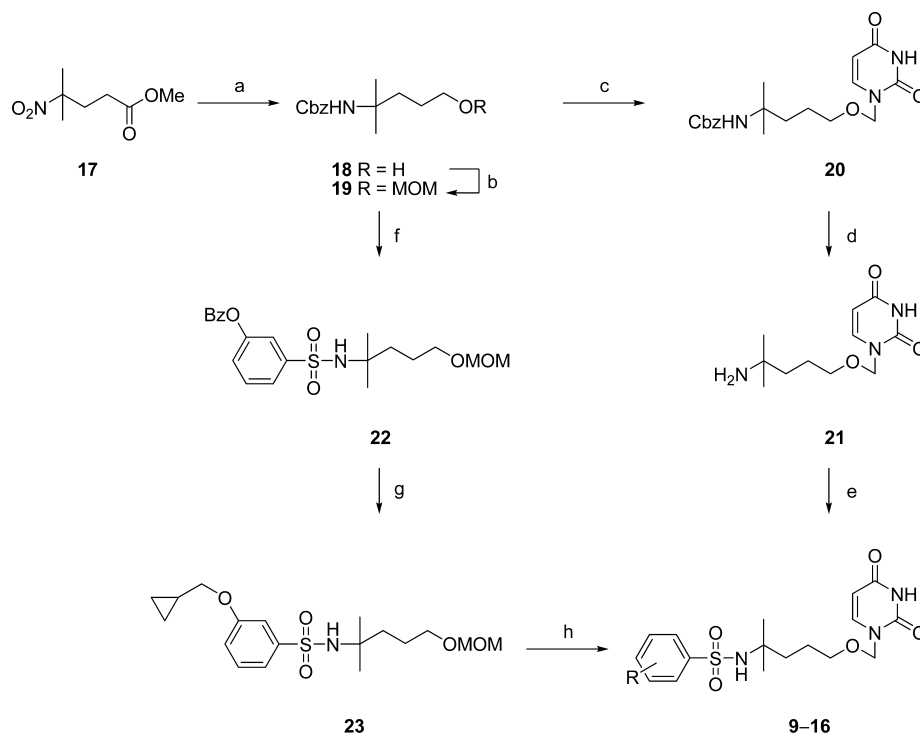
Figure 5. A proposed dUTPase inhibition mechanism by compound **9**.

Scheme 1. Synthesis of Compound 9–16[a]

[a]Reagents and conditions: (a) (1) 2.4 M LiAlH$_4$, THF, 45 °C, 16 h, (2) N-carbobenzoxyoxysuccinimide, CH$_2$Cl$_2$, 4 h; (b) MOMCl, N,N-diisopropylehtylamine, CH$_2$Cl$_2$, room temp, 2 h; (c) (1) 1.0 M BCl$_3$ in CH$_2$Cl$_2$, CH$_2$Cl$_2$, room temp, 2 h, (2) (TMS)$_2$uracil, I$_2$, 1,2-dichloroethane, reflux, 1.5 h; (d) H$_2$, 10%Pd/C, MeOH, room temp, 4 h; (e) RSO$_2$Cl, Et$_3$N, CH$_2$Cl$_2$, room temp, 16 h; (f) (1) H$_2$, 10%Pd/C, MeOH, room temp, 14 h, (2) 3-BzOPhSO$_2$Cl, Et$_3$N, CH$_2$Cl$_2$, room, temp, 2 h; (g) (1) 40% MeNH$_2$ in MeOH, room temp, 20 min, (2) (bromomethyl)cyclopropane, K$_2$CO$_3$, DMF, 90 °C, 16 h; (h) (1) 1.0 M BCl$_3$ in CH$_2$Cl$_2$, CH$_2$Cl$_2$, room temp, 1.5 h, (2) (TMS)$_2$uracil, I$_2$, 1,2-dichloroethane, reflux, 3 h.

alkylation of the resulting phenol moiety, and coupling with (TMS)$_2$uracil after activation of the MOM group with BCl$_3$.
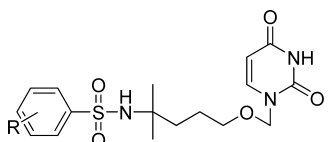
It was found that introduction of a substituent (chloro or methoxy group) at the *m*-position of the terminal phenyl ring of **9** retained or enhanced its enzyme inhibition activity compared with the unsubstituted compound **9** (Table 2). Among them, compound **11** with its *m*-methoxy group showed more potent inhibition (IC$_{50}$ = 1.2 μM) than **9**. All compounds enhanced the growth inhibition activity of FdUrd (1 μM) in HeLa S3 cells (Table 2). The EC$_{50}$ value of these compounds significantly correlated with their enzyme inhibition activity, indicating that the degree of reduction in the cellular dUTPase

level could be responsible for the enhancement of the growth inhibition of FdUrd.

Compound **16**, containing a cyclopropylmethoxy group at the *m*-position, exhibited an approximately 110-fold increase in potency (IC$_{50}$ = 0.035 μM) compared with the lead compound **9**. Introduction of a cyclopropylmethoxy group at the *m*-position of the terminal phenyl ring may enhance the hydrophobic interaction between the compound and enzyme.

Improvement of the Lead Compound 9 Part 2: Exploration of Another Linker Moiety. Although compound **16** has favorable biological activity, it could not be solidified, making it unsuitable as a drug candidate. In addition,

Table 2. Substitution Effects at the Terminal Phenyl Ring of Compound 9 on Human dUTPase Inhibition Activity

compd	R	IC$_{50}$ (μM)^a	EC$_{50}$ (μM)^b
9	H	3.9 ± 0.63	5.1 ± 0.32
10	o-CH$_3$O, p-Me	19.5 ± 2.8	14.1 ± 0.64
11	m-CH$_3$O	1.2 ± 0.08	1.1 ± 0.07
12	p-CH$_3$O	18.2 ± 1.4	14.9 ± 1.7
13	o-Cl	9.4 ± 0.34	7.93 ± 0.29
14	m-Cl	4.5 ± 0.29	3.96 ± 0.11
15	p-Cl	5.7 ± 0.32	4.97 ± 0.35
16	m-cyclopropylmethoxy	0.035 ± 0.002	0.18 ± 0.01

^{a}Concentration of each compound required to inhibit 50% of the amount of [5-^{3}H]dUMP produced by human dUTPase. ^{b}Concentration of each compound that reduces the T/C (%) value of FdUrd (1 μM) against HeLa S3 to half in 24 h. In all cases, IC$_{50}$ and EC$_{50}$ data represent the average of three independent assays, and errors are given as standard deviations.

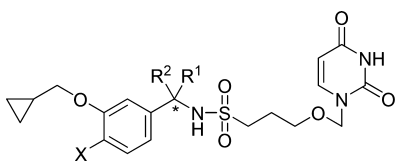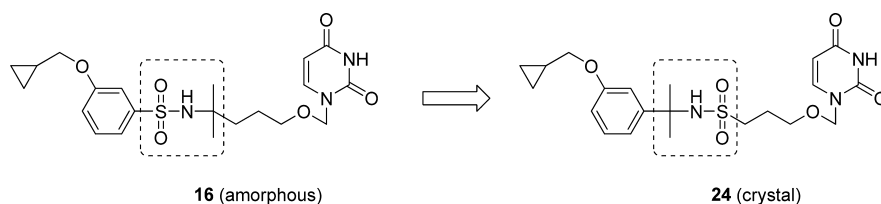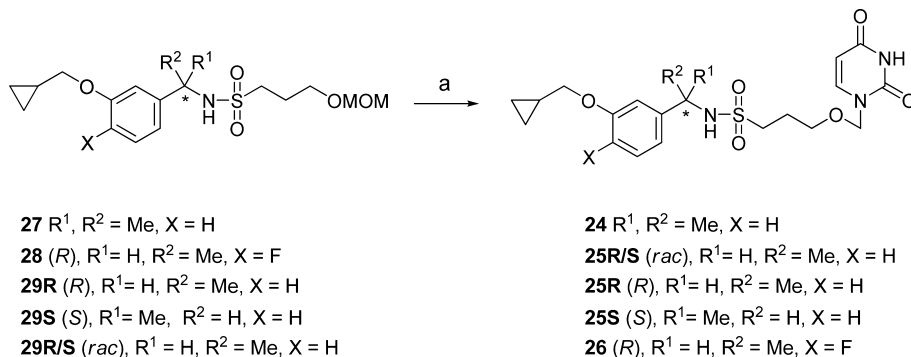**16 (amorphous)**   **24 (crystal)**

Figure 6. Compound 24 showed good physicochemical property in our chemical series.

Table 3. Biological Data of Compounds 24, 25R/S, 25R, 25S, and 26

compd	R^1	R^2	stereo	X	IC$_{50}$ (μM)^a	EC$_{50}$ (μM)^b
24	Me	Me		H	0.34 ± 0.03	0.45 ± 0.06
25R/S	Me	H	rac	H	0.062 ± 0.001	0.14 ± 0.01
25R	Me	H	R	H	0.040 ± 0.007	0.066 ± 0.005
25S	H	Me	S	H	2.5 ± 0.34	4.15 ± 0.57
26	Me	H	R	F	0.021 ± 0.003	0.075 ± 0.002

^{a}Concentration of each compound required to inhibit 50% of the amount of [5-^{3}H]dUMP produced by human dUTPase. ^{b}Concentration of each compound that reduces the T/C (%) value of FdUrd (1 μM) against HeLa S3 to half in 24 h. In all cases, IC$_{50}$ and EC$_{50}$ data represent the average of three independent assays, and errors are given as standard deviations.

Scheme 2. Synthesis of Compounds 24, 25R/S, 25R, 25S, and 26^a

27 R^1, R^2 = Me, X = H   **24** R^1, R^2 = Me, X = H
28 (R), R^1 = H, R^2 = Me, X = F   **25R/S** (rac), R^1 = H, R^2 = Me, X = H
29R (R), R^1 = H, R^2 = Me, X = H   **25R** (R), R^1 = H, R^2 = Me, X = H
29S (S), R^1 = Me, R^2 = H, X = H   **25S** (S), R^1 = Me, R^2 = H, X = H
29R/S (rac), R^1 = H, R^2 = Me, X = H   **26** (R), R^1 = H, R^2 = Me, X = F

^{a}Reagents and conditions: (a) (1) 1.0 M BCl$_3$ in CH$_2$Cl$_2$, CH$_2$Cl$_2$, room temp, 1.5 h, (2) (TMS)$_2$uracil, I$_2$, 1,2-dichloroethane, reflux, 3 h.

analogues of compound **9** such as compounds **10−15** had similar unfavorable physicochemical properties. Thus, we designed additional novel compounds with an alternative linker to improve physicochemical properties and found that compound **24** was easily solidified (Figure 6). Hence, although compound **24** had slightly less enzyme inhibition activity (IC$_{50}$ = 0.34 μM) than compound **16**, we selected **24** as an alternative lead compound.

To investigate the substituent effect at the *p*-position of the terminal phenyl ring and the dimethyl group at the benzyl position of compound **24** on the enzyme inhibition activity, we synthesized monomethyl compounds **25R/S**, **25R**, **25S**, and **26** (Table 3). Procedures for the synthesis of compounds **27**, **28**, **29R**, **29S**, and **29R/S** are detailed in the Supporting Information. These compounds were activated with BCl$_3$ and then reacted with (TMS)$_2$uracil to give target analogues **24**, **25R/S**, **25R**, **25S**, and **26** (Scheme 2).

Racemic monomethyl compound **25R/S** showed markedly increased inhibition activity against human dUTPase (IC$_{50}$ = 0.062 μM). Therefore, we further synthesized the *S*- and *R*-enantiomers at the benzyl position of compound **25R/S** to identify the eutomer. *R*-Enantiomer **25R** was revealed to be the eutomer (IC$_{50}$ = 0.040 μM), and the eudismic ratio was relatively large. This large eudismic ratio suggested that the (*R*)-asymmetric center may be essential for the bioactive form, and the terminal phenyl moiety of the inhibitors plays an important role in the pharmacophore.

We further found that compound **26**, which has an introduced fluorine moiety at the *p*-position of the terminal phenyl group of compound **25R**, also exhibit highly potent enzyme inhibition activity (IC$_{50}$ = 0.021 μM) and highly potent enhancement of the growth inhibition activity of FdUrd in vitro (EC$_{50}$ = 0.075 μM). Compound **26** alone had little effect on cell growth (IC$_{50}$ = 28.3 μM).

In Vivo Pharmacokinetics (PK) Profile of Compound 26. We selected compound **26** because of its in vitro potency and evaluated preliminary pharmacokinetics (PK) profile in mice (Table 4). Compound **26** was well absorbed after oral

Table 4. Pharmacokinetic Profile of 26 after Oral Administration (po)[a]

	AUC$_{0-t}$ (μM·h)	C$_{max}$ (μM)	T$_{1/2}$ (h)	T$_{max}$ (h)
26	24.9	15.1	1.4	0.5

[a]Balb/cA male mice (*n* = 2) was dosed at 50 mg/kg. The po formulation contained 2.5% DMA, 2.5% Tween 80, and 10% Cremophor EL.

administration in mice plasma. These PK data showed that compound **26** has a favorable profile for in vivo study.

Enhancing Activity of Compound 26 for Antitumor Effect of 5-FU against the MX-1 Breast Cancer Xenograft Model in Mice. Compound **26** (300 mg/kg/day) was administered orally in combination with continuous infusion of 5-FU (15 mg/kg/day) against the MX-1 xenograft model in mice. Compound **26** showed significant potency (IR = 83%) in enhancing the antitumor effect of 5-FU (Table 5, Figure 7A).
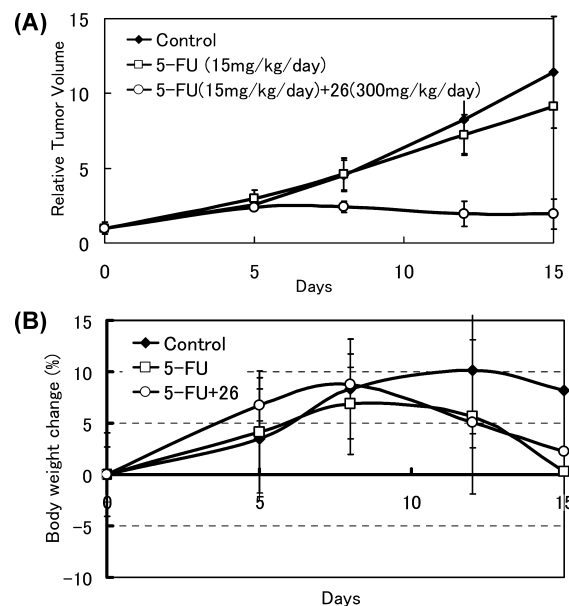
Figure 7. (A) Antitumor activity of **26** in combination with 5-FU in the MX-1 xenograft model. Relative tumor volume (RTV) is expressed as mean ± SD of at least three independent experiments. (B) Body weight change (%) is expressed as mean ± SD.

Although 5-FU treatment at 15 mg/kg/day had little antitumor effect, combination with **26** completely prevented the tumor growth without significant weight loss, as compared with the vehicle-treated group (Figure 7B). Compound **26** alone exhibited no antitumor activity in vivo (Table 5). This is the first in vivo evidence of a human dUTPase inhibitor enhancing the antitumor activity of a TS inhibitor.

■ **CONCLUSION**

We have described the discovery of a novel class of human dUTPase inhibitors. Starting from low affinity ligand **7**, we developed compound **9** whose terminal phenyl ring is located in a position similar to that of Phe158 in the active form and which mimics the stacked mode of the uracil ring of the substrate dUTP with that of Phe158. Further SAR studies of compound **9** led to compound **26** that has the greatest in vitro

Table 5. Antitumor Activity of Compound 26 in Combination with 5-FU in the MX-1 Xenograft Model

drug	dose (mg/kg/day)	treatment	TV[a] (mm^3, mean ± SD)	RTV[b] (mean ± SD)	IR[c] (%)
control			2048 ± 693.7	11.4 ± 3.74	
5-FU	15	CI	1645 ± 322.6	9.13 ± 1.35	20
26	300	po	2698 ± 764.6	14.9 ± 3.88	−30.9
5-FU/**26**	15/300	CI/po	299.7 ± 204.3	1.94 ± 1.01**,##[d,e]	83.0

[a]Tumor volume (TV) on day 15 was calculated according to the following formula: TV (mm^3) = (width)^2 × (length)/2. [b]Relative tumor volume (RTV) on day 15 was calculated as the ratio of TV on day 15 to that on day 0 according to the following formula: RTV = (TV on day 15)/(TV on day 0). [c]Inhibition rate (IR) of tumor growth on day 15 on the basis of RTV was calculated according to the following formula: IR (%) = [1 − (mean RTV of the treated group)/(mean RTV of the control group)] × 100. [d]**p < 0.01 Dunnet test as compared with the control group. [e]**p < 0.01 Student's *t* test as compared with the 5-FU group.

potency (IC$_{50}$ = 0.021 μM, EC$_{50}$ = 0.075 μM) reported to date. Furthermore, compound **26** displayed drastic tumor growth inhibition when combined with 5-FU against the MX-1 xenograft model in mice. On the basis of these findings, we expect that human dUTPase inhibitors will ultimately lead to the establishment of a landmark cancer therapeutic strategy, providing hope for cancer patients.

■ EXPERIMENTAL SECTION

Chemistry. All commercially available reagents and solvents were used without further purification unless otherwise specified. All reactions were performed under an inert nitrogen atmosphere unless otherwise specified. ^{1}H NMR spectra were recorded on a JEOL JNM-EX-270 (270 MHz) or JEOL JNM-LA-400 (400 MHz) spectrometer, and ^{13}C NMR spectra were recorded on a JEOL JNM-LA-400 (100 MHz) spectrometer. Chemical shifts were given in parts per million (ppm, δ) with tetramethylsilane as the internal standard, and coupling constant (*J* value) is given in hertz (Hz). Splitting patterns and apparent multiplicities are designated as s, singlet; d, doublet; dd, double doublet; t, triplet; dt, doublet triplet; q, quartet; quin, quintet; m, multiplet; brs, broad singlet. Analytical thin layer chromatography (TLC) was performed on silica gel 60 F$_{254}$ precoated plates (Merck). Column chromatography was performed on Merck silica gel 60 (230–400 mesh). Optical rotation was determined using Horiba SEPA-200 polarimeter. High-resolution mass spectra (HRMS) was recorded either on JEOL JMS-700 (FAB) or on Waters micromass Q-Tof-2 (TOF). The purity of all final compounds was determined by combustion analysis or high pressure liquid chromatography (HPLC); purity of at least 95% was found. Elemental analyses were performed using a Thermo Electron Corporation Flash EA 1112 series. Analytical HPLC was performed on a Shimazu Prominence system using L-column 2 ODS column (4.6 mm × 150 mm, 3 μm) with an 8 min linear gradient from 10–80% acetonitrile/10 mM phosphate buffer (pH 6.5) and a flow rate of 1.3 mL/min with UV detection at 220 nm (method A) and a Shim-pack XR-ODS column (3.0 mm × 50 mm, 2.2 μm) with an 8 min linear gradient of 10–80% acetonitrile/10 mM phosphate buffer (pH 6.5) and a flow rate of 0.8 mL/min with UV detection at 220 nm (method B). The retention time of compound peak in HPLC was denoted t_R.

Benzyl 5-Hydroxy-2-methylpentan-2-ylcarbamate (18). To a stirred solution of LiAlH$_4$ in THF (2.4 M, 71 mL, 170 mmol) was slowly added a solution of methyl 4-methyl-4-nitropentanoate **17** (10.0 g, 57.1 mmol) over 30 min at room temperature, and the mixture was stirred at 45 °C for 16 h. The reaction mixture was cooled to 0 °C, and H$_2$O was then added dropwise. The resultant precipitate was removed by filtration and washed with MeOH (100 mL) and THF (900 mL). The combined filtrate was concentrated under reduced pressure. The residue was dissolved in CH$_2$Cl$_2$ (100 mL). To the mixture was added *N*-carbobenzoxyoxysuccinimide (18.0 g, 72.7 mmol), and the resulting mixture was stirred at room temperature for 4 h. The reaction mixture was concentrated under reduced pressure, and the residue was purified by column chromatography on silica gel eluting with (hexane/EtOAc = 1/1) to afford the title compound (14.0 g, 55.7 mmol, 98%) as a colorless oil. ^{1}H NMR (270 MHz, CDCl$_3$) δ 1.11 (6H, s), 1.50–1.61 (4H, m), 3.57–3.65 (2H, m), 4.71 (1H, brs), 5.21 (2H, s), 7.33–7.39 (5H, m). HRMS (FAB) calcd for C$_{14}$H$_{22}$NO$_3$ [M + H]$^+$ 252.1600, found 252.1593.

Benzyl 5-(Methoxymethoxy)-2-methylpentan-2-ylcarbamate (19). To a stirred solution of **18** (14.0 g, 55.7 mmol) in CH$_2$Cl$_2$ (100 mL) was added *N*,*N*-diisopropylethylamine (20 mL, 115 mmol) and MOMCl (4.7 mL, 61.9 mmol) at room temperature, and the resulting mixture was stirred at room temperature for 2 h. The mixture was poured into satd aq NH$_4$Cl and extracted with CHCl$_3$ two times. The combined organic layer was washed with satd aq NH$_4$Cl and brine, dried over Na$_2$SO$_4$, filtered, and concentrated under reduced pressure. The residue was purified by column chromatography on silica gel eluting with (hexane/EtOAc = 7/3) to afford the title compound (8.80 g, 29.8 mmol, 54%) as a colorless oil. ^{1}H NMR (270 MHz, CDCl$_3$) δ 1.31 (6H, s), 1.57–1.62 (2H, m), 1.69–1.73

(2H, m), 3.35 (3H, s), 3.51 (2H, t, *J* = 6.2 Hz), 4.61 (2H, s), 4.71 (1H, brs), 5.05 (2H, s), 7.30–7.36 (5H, m). HRMS (FAB) calcd for C$_{16}$H$_{24}$NO$_4$ [M − H]$^-$ 294.1705, found 294.1732.

Benzyl 5-((2,4-Dioxo-3,4-dihydropyrimidin-1(2*H*)-yl)-methoxy)-2-methylpentan-2-ylcarbamate (20). To a stirred solution of **19** (369 mg, 1.25 mmol) in CH$_2$Cl$_2$ (1.0 mL) was gradually added BCl$_3$ in CH$_2$Cl$_2$ (1.0 M, 330 μL, 0.33 mmol) at 0 °C, and the resulting mixture was stirred at room temperature for 2 h. The reaction mixture was concentrated under reduced pressure, and the residue was then dissolved in 1,2-dichloroethane (10 mL). To the mixture was added 2,4-bis(trimethylsilyloxy)pyrimidine (256 mg, 1.00 mmol) and iodine (10.0 mg, 0.039 mmol) at room temperature, and the mixture was heated to reflux at 93 °C for 1.5 h. The reaction mixture was cooled to room temperature, satd aq Na$_2$S$_2$O$_3$ solution (10 mL) was then added, and the resulting mixture was extracted with ethyl acetate (30 mL) two times. The combined organic layer was washed with brine, dried over Na$_2$SO$_4$, filtered, and concentrated under reduced pressure. The residue was purified by column chromatography on silica gel eluted with (CHCl$_3$/MeOH = 19/1) followed by C$_{18}$ reverse-phase column chromatography eluted with (MeOH/H$_2$O = 1/1) to obtain the title compound (206 mg, 0.55 mmol, 44%) as a colorless gum. ^{1}H NMR (270 MHz, CDCl$_3$) δ 1.28 (6H, s), 1.52–1.61 (2H, m), 1.63–1.74 (2H, m), 3.52 (2H, t, *J* = 5.9 Hz), 4.75 (1H, brs), 5.04 (2H, s), 5.10 (2H, s), 5.75 (1H, d, *J* = 8.1 Hz), 7.26–7.36 (6H, m). HRMS (FAB) calcd for C$_{19}$H$_{26}$N$_3$O$_5$ [M + H]$^+$ 376.1872, found 376.1881.

1-((4-Amino-4-methylpentyloxy)methyl)pyrimidine-2,4-(1*H*,3*H*)-dione (21). A mixture of **20** (120 mg, 0.32 mmol) and 10% palladium on activated carbon (30.0 mg) in MeOH (4.0 mL) was stirred at room temperature for 4 h under a hydrogen atmosphere. The precipitate was removed by filtration through a pad of Celite and washed with MeOH. The combined filtrate was concentrated under reduced pressure to afford crude amine (77.5 mg, quant.). The crude amine **21** was used for the next step without further purification. ^{1}H NMR (270 MHz, DMSO-d_6) δ 0.97 (6H, s), 1.20–1.27 (2H, m), 1.47–1.53 (2H, m), 3.16–3.46 (2H, m), 3.95 (2H, brs), 5.05 (2H, s), 5.59 (1H, dt, *J* = 8.0, 1.8 Hz), 7.67 (1H, dt, *J* = 8.0, 1.8 Hz). HRMS (FAB) calcd for C$_{11}$H$_{20}$N$_3$O$_3$ [M + H]$^+$ 242.1505, found 242.1542.

N-(5-((2,4-Dioxo-3,4-dihydropyrimidin-1(2*H*)-yl)methoxy)-2-methylpentan-2-yl)benzenesulfonamide (9). To a stirred solution of **21** (45.0 mg, 0.19 mmol) in CH$_2$Cl$_2$ (1.5 mL) was added Et$_3$N (34 μL, 0.24 mmol) and benzenesulfonyl chloride (28 μL, 0.22 mmol) at 0 °C, and the resulting mixture was stirred at room temperature for 16 h. The mixture was poured into H$_2$O and extracted with EtOAc two times. The combined organic layer was washed with brine, dried over Na$_2$SO$_4$, filtered, and concentrated under reduced pressure. The residue was purified by column chromatography on silica gel eluting with (EtOAc) to afford the title compound (40.1 mg, 0.11 mmol, 56%) as a colorless gum. ^{1}H NMR (270 MHz, DMSO-d_6) δ 1.01 (6H, s), 1.34–1.46 (4H, m), 3.26–3.32 (2H, m), 5.00 (2H, s), 5.60 (1H, d, *J* = 7.8 Hz), 7.41 (1H, brs), 7.49–7.54 (3H, m), 7.64 (1H, d, *J* = 7.8 Hz), 7.78–7.81 (2H, m), 11.30 (1H, brs). ^{13}C NMR (100 MHz, CDCl$_3$) δ 23.8, 27.5, 39.2, 56.6, 69.5, 76.6, 103.1, 126.5, 128.8, 132.1, 143.4, 143.5, 151.2, 163.8. Anal. Calcd for C$_{17}$H$_{23}$N$_3$O$_5$S: C, 53.53; H, 6.08; N, 11.02. Found: C, 53.94; H, 6.27; N, 11.07.

N-(5-((2,4-Dioxo-3,4-dihydropyrimidin-1(2*H*)-yl)methoxy)-2-methylpentan-2-yl)-2-methoxy-4-methylbenzenesulfonamide (10). 10 was prepared from **21** (45.1 mg, 0.19 mmol) as described for the preparation of **9**; white foam (22.1 mg, 0.052 mmol, 27%). ^{1}H NMR (400 MHz, CD$_3$OD) δ 1.08 (6H, s), 1.43–1.49 (2H, m), 1.52–1.56 (2H, m), 2.41 (3H, s), 3.37–3.40 (2H, m), 3.93 (3H, s), 5.10 (2H, s), 5.69 (1H, d, *J* = 7.8 Hz), 6.84–6.87 (1H, m), 6.97–6.99 (1H, m), 7.60 (1H, d, *J* = 8.0 Hz), 7.66 (1H, d, *J* = 7.8 Hz). ^{13}C NMR (100 MHz, CDCl$_3$) δ 21.9, 23.9, 27.6, 39.1, 56.1, 56.4, 69.7, 76.7, 103.1, 112.8, 121.5, 128.5, 129.1, 143.2, 145.1, 150.8, 155.8, 163.0. Anal. Calcd for C$_{19}$H$_{27}$N$_3$O$_6$S·0.3H$_2$O: C, 52.96; H, 6.46; N,9.75. Found: C, 52.99; H, 6.31; N, 9.47.

N-(5-((2,4-Dioxo-3,4-dihydropyrimidin-1(2*H*)-yl)methoxy)-2-methylpentan-2-yl)-3-methoxybenzenesulfonamide (11). 11 was prepared from **21** (45.0 mg, 0.19 mmol) as described for the

preparation of **9**; white foam (30.0 mg, 0.073 mmol, 38%). ^{1}H NMR (400 MHz, CD$_3$OD) δ 1.12 (6H, s), 1.46−1.54 (4H, m), 3.37−3.41 (2H, m), 3.84 (3H, s), 5.10 (2H, s), 5.70 (1H, d, J = 7.9 Hz), 7.09−7.14 (1H, m), 7.39−7.43 (3H, m), 7.60 (1H, d, J = 7.9 Hz). ^{13}C NMR (100 MHz, CDCl$_3$) δ 23.9, 27.6, 39.3, 55.6, 56.8, 69.6, 76.7, 103.2, 111.8, 118.3, 119.1, 130.0, 143.2, 144.6, 150.9, 159.7, 163.1; Anal. Calcd for C$_{18}$H$_{25}$N$_3$O$_6$S: C, 52.54; H, 6.12; N, 10.21. Found: C, 52.35; H, 6.30; N, 9.98.

N-(5-((2,4-Dioxo-3,4-dihydropyrimidin-1(2H)-yl)methoxy)-2-methylpentan-2-yl)-4-methoxybenzenesulfonamide (12). 12 was prepared from **21** (30.1 mg, 0.12 mmol) as described for the preparation of **9**; white foam (35.2 mg, 0.086 mmol, 72%). ^{1}H NMR (270 MHz, CD$_3$OD) δ 1.08 (6H, s), 1.46−1.56 (4H, m), 3.40−3.44 (2H, m), 3.86 (3H, s), 5.10 (2H, s), 5.70 (1H, d, J = 7.9 Hz), 7.03 (1H, dd, J = 6.8, 2.0 Hz), 7.60 (2H, d, J = 7.9 Hz), 7.78 (2H, dd, J = 6.8, 2.0 Hz). ^{13}C NMR (100 MHz, CDCl$_3$) δ 23.9, 27.7, 39.3, 55.6, 56.5, 69.6, 76.7, 103.2, 114.1, 129.0, 135.2, 143.3, 151.0, 162.5, 163.3. Anal. Calcd for C$_{18}$H$_{25}$N$_3$O$_6$S·0.5H$_2$O: C, 51.42; H, 6.23; N, 9.99. Found: C, 51.74; H, 6.01; N, 9.80.

2-Chloro-N-(5-((2,4-dioxo-3,4-dihydropyrimidin-1(2H)-yl)-methoxy)-2-methylpentan-2-yl)benzenesulfonamide (13). 13 was prepared from **21** (45.3 mg, 0.19 mmol) as described for the preparation of **9**; white foam (24.3 mg, 0.058 mmol, 31%). ^{1}H NMR (270 MHz, CD$_3$OD) δ 1.11 (6H, s), 1.50−1.59 (4H, m), 3.40−3.43 (2H, m), 5.10 (2H, s), 5.70 (1H, d, J = 7.8 Hz), 7.44−7.47 (1H, m), 7.50−7.62 (3H, m), 8.04−8.07 (1H, m). ^{13}C NMR (100 MHz, CDCl$_3$) δ 23.9, 27.5, 39.2, 57.0, 69.6, 76.7, 103.2, 127.3, 130.4, 131.2, 131.4, 133.2, 140.7, 143.2, 150.8, 163.0. Anal. Calcd for C$_{17}$H$_{22}$ClN$_3$O$_5$S·H$_2$O: C, 47.06; H, 5.58; N, 9.68. Found: C, 47.36; H, 5.22; N, 9.49.

3-Chloro-N-(5-((2,4-dioxo-3,4-dihydropyrimidin-1(2H)-yl)-methoxy)-2-methylpentan-2-yl)benzenesulfonamide (14). 14 was prepared from **21** (30.3 mg, 0.13 mmol) as described for the preparation of **9**; white foam (26.8 mg, 0.064 mmol, 49%). ^{1}H NMR (270 MHz, CD$_3$OD) δ 1.13 (6H, s), 1.52−1.55 (4H, m), 3.41−3.46 (2H, m), 5.11 (2H, s), 5.70 (1H, d, J = 7.9 Hz), 7.53−7.63 (3H, m), 7.82−7.86 (2H, m). ^{13}C NMR (100 MHz, CDCl$_3$) δ 23.9, 27.7, 39.3, 57.0, 69.5, 76.7, 103.3, 125.0, 127.0, 130.3, 132.3, 135.0, 143.3, 145.3, 151.1, 163.5. HRMS (TOF) calcd for C$_{17}$H$_{23}$ClN$_3$O$_5$S [M + H]$^+$ 416.1047, found 416.1048. HPLC purity: method B = 99.3%, t_R = 5.28 min.

4-Chloro-N-(5-((2,4-dioxo-3,4-dihydropyrimidin-1(2H)-yl)-methoxy)-2-methylpentan-2-yl)benzenesulfonamide (15). 15 was prepared from **21** (45.3 mg, 0.19 mmol) as described for the preparation of **9**; white foam (34.1 mg, 0.082 mmol, 43%). ^{1}H NMR (270 MHz, CD$_3$OD) δ 1.12 (6H, s), 1.45−1.54 (4H, m), 5.11 (2H, s), 5.69 (1H, d, J = 7.8 Hz), 7.52−7.55 (2H, m), 7.60 (1H, d, J = 7.8 Hz), 7.82−7.85 (2H, m). ^{13}C NMR (100 MHz, CDCl$_3$) δ 23.9, 27.7, 39.4, 56.9, 69.5, 76.7, 103.3, 128.4, 129.2, 138.6, 142.0, 143.4, 150.9, 163.1. Anal. Calcd for C$_{17}$H$_{22}$ClN$_3$O$_5$S·0.5H$_2$O: C, 48.05; H, 5.46; N, 9.89. Found: C, 47.75; H, 5.17; N, 9.69.

3-(N-(5-(Methoxymethyl)-2-methylpentan-2-yl)sulfamoyl)-phenyl benzoate (22). A mixture of **19** (586 mg, 2.00 mmol) and 10% palladium on activated carbon (330 mg) in MeOH (7.0 mL) was stirred at room temperature for 14 h under a hydrogen atmosphere. The precipitate was removed by filtration through a pad of Celite and washed with MeOH. The combined filtrate was concentrated under reduced pressure, and the residue was coevaporated with THF two times.

To a solution of the above residue in CH$_2$Cl$_2$ (4.0 mL) was added Et$_3$N (362 μL, 2.60 mmol) and 3-(chlorosulfonyl)phenyl benzoate (682 mg, 2.30 mmol) at 0 °C, and the resulting mixture was stirred at room temperature for 2 h. The mixture was poured into H$_2$O and extracted with EtOAc two times. The combined organic layer was washed with brine, dried over Na$_2$SO$_4$, and concentrated under reduced pressure. The residue was purified by column chromatography on silica gel eluting with (hexane/EtOAc = 3/1) to afford the title compound (630 mg, 1.49 mmol, 75% from **19**) as a colorless oil. ^{1}H NMR (270 MHz, DMSO-d$_6$) δ 1.07 (6H, s), 1.45−1.52 (4H, m), 3.20 (3H, s), 3.32−3.40 (2H, m), 4.48 (2H, s), 7.52−7.79 (8H, m),

8.13−8.17 (2H, m). HRMS (FAB) calcd for C$_{21}$H$_{26}$NO$_6$S [M − H]$^-$ 420.1481, found 420.1511.

3-(Cyclopropylmethoxy)-N-(5-(methoxymethyl)-2-methyl-pentan-2-yl)benzenesulfonamide (23). A solution of **22** (630 mg, 1.49 mmol) in 40% MeNH$_2$ in MeOH (4.0 mL) was stirred at room temperature for 20 min. The mixture was concentrated under reduced pressure, and the residue was coevaporated with toluene two times. This residue was dissolved in DMF (4.0 mL). To the mixture was added K$_2$CO$_3$ (373 mg, 2.70 mmol) and (bromomethyl)cyclopropane (156 μL, 1.61 mmol) at room temperature. The resulting mixture was stirred at 90 °C for 16 h. After cooling to room temperature, the mixture was poured into H$_2$O, extracted with EtOAc two times. The combined organic layer was washed with brine, dried over Na$_2$SO$_4$, and concentrated under reduced pressure. The residue was purified by column chromatography on silica gel eluting with (hexane/EtOAc = 4/1) to afford the title compound (405 mg, 1.09 mmol, 73%) as a colorless oil. ^{1}H NMR (270 MHz, DMSO-d$_6$) δ 0.30−0.36 (2H, m), 0.53−0.60 (2H, m), 1.04 (6H, s), 1.18−1.24 (1H, m), 1.40−1.48 (4H, m), 3.20 (3H, s), 3.26−3.34 (2H, m), 3.85 (2H, d, J = 6.8 Hz), 4.48 (2H, s), 7.11−7.14 (1H, m), 7.31−7.47 (4H, m). HRMS (FAB) calcd for C$_{18}$H$_{28}$NO$_5$S [M − H]$^-$ 370.1688, found 370.1716.

3-(Cyclopropylmethoxy)-N-(5-((2,4-dioxo-3,4-dihydropyri-midin-1(2H)-yl)methoxy)-2-methylpentan-2-yl)-benzenesulfonamide (16). To a stirred solution of **23** (120 mg, 0.32 mmol) in CH$_2$Cl$_2$ (500 μL) was added BCl$_3$ in CH$_2$Cl$_2$ (1.0 M, 120 μL, 0.12 mmol) at 0 °C, and the resulting mixture was stirred at room temperature for 1.5 h. The mixture was concentrated under reduced pressure, and the residue was dissolved in 1,2-dichloroethane (2.0 mL). The mixture was then added to a mixture of 2,4-bis(trimethylsilyloxy)pyrimidine (124 mg, 0.48 mmol) and iodine (3.0 mg, 0.012 mmol) in 1,2-dichloroethane (1.0 mL) at room temperature. The resultant mixture was heated to reflux at 95 °C for 3 h. After cooling to room temperature, the mixture was poured into H$_2$O and extracted with CHCl$_3$ two times. The combined organic layer was washed with satd aq Na$_2$S$_2$O$_3$, brine, dried over Na$_2$SO$_4$, filtered, and concentrated under reduced pressure. The residue was purified by column chromatography on silica gel eluting with (EtOAc) to afford the title compound (109 mg, 0.24 mmol, 75%) as a white foam. ^{1}H NMR (270 MHz, DMSO-d$_6$) δ 0.30−0.34 (2H, m), 0.53−0.58 (2H, m), 1.01 (6H, s), 1.15−1.24 (1H, m), 1.36−1.48 (4H, m), 3.32−3.39 (2H, m), 3.85 (2H, d, J = 6.9 Hz), 5.00 (2H, s), 5.60 (1H, d, J = 7.8 Hz), 7.09−7.13 (1H, m), 7.30−7.45 (4H, m), 7.64 (1H, d, J = 7.8 Hz), 11.3 (1H, brs). ^{13}C NMR (100 MHz, CDCl$_3$) δ 3.2, 10.0, 23.9, 27.5, 39.3, 56.6, 69.5, 73.1, 103.1, 112.3, 118.8, 119.0, 129.9, 143.4, 144.6, 151.2, 159.1, 163.7. Anal. Calcd for C$_{21}$H$_{29}$N$_3$O$_6$S·H$_2$O: C, 53.72; H, 6.65; N, 8.95. Found: C, 54.09; H, 6.33; N, 8.96.

N-(2-(3-(Cyclopropylmethoxy)phenyl)propan-2-yl)-3-((2,4-dioxo-3,4-dihydropyrimidin-1(2H)-yl)methoxy)propane-1-sul-fonamide (24). 24 was prepared from **27** (6.72 g, 18.1 mmol) as described for the preparation of **16**; white solid (3.38 g, 7.49 mmol, 41%). ^{1}H NMR (270 MHz, CDCl$_3$) δ 0.30−0.35 (2H, m), 0.62−0.73 (2H, m), 1.22−1.31 (1H, m), 1.74 (6H, s), 1.96−2.08 (2H, m), 2.81 (2H, t, J = 7.0 Hz), 3.55−3.62 (2H, m), 3.81 (2H, d, J = 7.6 Hz), 4.63 (1H, brs), 5.10 (2H, s), 5.76 (1H, dd, J = 7.8, 1.1 Hz), 6.76−6.88 (1H, m), 7.05−7.10 (2H, m), 7.24−7.30 (2H, m), 8.35 (1H, brs). ^{13}C NMR (100 MHz, DMSO-d$_6$) δ 3.1, 10.1, 23.9, 29.8, 51.3, 57.2, 66.4, 71.9, 76.2, 101.6, 112.0, 112.5, 117.6, 128.9, 144.8, 148.6, 151.0, 158.3, 163.6. Anal. Calcd for C$_{21}$H$_{29}$N$_3$O$_6$S: C, 55.86; H, 6.47; N, 9.31. Found: C, 55.55; H, 6.50; N, 9.30.

N-(1-(3-(Cyclopropylmethoxy)phenyl)ethyl)-3-((2,4-dioxo-3,4-dihydropyrimidin-1(2H)-yl)methoxy)propane-1-sulfona-mide (25R/S). 25R/S was prepared from **29R/S** (548 mg, 1.53 mmol) as described for the preparation of **16**; colorless gum (248 mg, 0.57 mmol, 37%). ^{1}H NMR (270 MHz, CDCl$_3$) δ 0.31−0.38 (2H, m), 0.59−0.69 (2H, m), 1.20−1.38 (1H, m), 1.52 (3H, d, J = 6.8 Hz), 1.80−1.98 (2H, m), 2.51−2.88 (2H, m), 3.49−3.53 (2H, m), 3.88 (2H, d, J = 7.0 Hz), 4.58 (1H, quin, J = 6.8 Hz), 4.84 (1H, d, J = 6.8 Hz), 5.06 (2H, s), 5.76 (1H, dd, J = 8.1, 2.2 Hz), 6.8−6.91 (3H, m), 7.21−7.29 (2H, m), 8.69 (1H, brs). ^{13}C NMR (100 MHz, DMSO-d$_6$) δ 3.0, 10.1, 23.6, 24.1, 49.1, 52.6, 66.3, 71.9, 76.1, 101.7, 112.3, 113.0, 118.1, 129.4, 144.7, 145.7, 151.0, 158.7, 163.6. Anal. Calcd for

$C_{20}H_{27}N_3O_6S$: C, 54.90; H, 6.22; N, 9.60. Found: C, 55.28; H, 6.25; N, 9.41.

(R)-N-(1-(3-(Cyclopropylmethoxy)phenyl)ethyl)-3-((2,4-dioxo-3,4-dihydropyrimidin-1(2H)-yl)methoxy)propane-1-sulfonamide (25R). 25R was prepared from 29R (219 mg, 0.61 mmol) as described for the preparation of 16; colorless gum (106 mg, 0.24 mmol, 39%). ^{1}H NMR (270 MHz, CDCl$_3$) δ 0.31−0.38 (2H, m), 0.59−0.67 (2H, m), 1.19−1.30 (1H, m), 1.52 (3H, d, J = 6.8 Hz), 1.78−2.00 (2H, m), 2.51−2.89 (2H, m), 3.44−3.59 (2H, m), 3.88 (2H, d, J = 7.0 Hz), 4.56 (1H, quin, J = 6.8 Hz), 5.06 (2H, s), 5.17 (1H, d, J = 6.8 Hz), 5.77 (1H, d, J = 7.8 Hz), 6.79−6.92 (3H, m), 7.20−7.28 (2H, m), 9.12 (1H, brs). ^{13}C NMR (100 MHz, CDCl$_3$) δ 3.2, 10.2, 10.7, 23.7, 30.7, 50.2, 59.6, 66.9, 72.8, 76.3, 103.1, 113.1, 113.7, 118.9, 129.8, 143.2, 151.1, 159.3, 163.7. Anal. Calcd for $C_{20}H_{27}N_3O_6S$: C, 54.90; H, 6.22; N, 9.60. Found: C, 54.71; H, 6.46; N, 9.57. $[\alpha]_D^{25}$ + 20.7 (c 1.00, MeOH).

(S)-N-(1-(3-(Cyclopropylmethoxy)phenyl)ethyl)-3-((2,4-dioxo-3,4-dihydropyrimidin-1(2H)-yl)methoxy)propane-1-sulfonamide (25S). 25S was prepared from 29S (530 mg, 1.48 mmol) as described for the preparation of 16; colorless gum (291 mg, 0.67 mmol, 45%). ^{1}H NMR (400 MHz, DMSO-d_6) δ 0.25−0.29 (2H, m), 0.50−0.55 (2H, m), 1.14−1.20 (1H, m), 1.32 (3H, d, J = 7.5 Hz), 1.66−1.75 (2H, m), 2.49−2.56 (1H, m), 2.73−2.80 (1H, m), 3.26−3.39 (2H, m), 3.75 (2H, d, J = 7.1 Hz), 4.33 (1H, quin, J = 7.5 Hz), 4.95 (2H, s), 5.57 (1H, d, J = 8.0 Hz), 6.74 (1H, dd, J = 8.3, 2.4 Hz), 6.85 (1H, d, J = 7.6 Hz), 6.90 (1H, s), 7.16 (1H, t, J = 8.1 Hz), 7.58 (1H, d, J = 8.0 Hz), 7.69 (1H, d, J = 8.5 Hz), 11.3 (1H, brs). ^{13}C NMR (100 MHz, DMSO-d_6) δ 3.1, 10.2, 23.7, 24.1, 49.2, 52.7, 66.3, 71.9, 76.1, 101.7, 112.3, 113.0, 118.2, 129.4, 144.8, 145.8, 151.1, 158.7, 163.7. Anal. Calcd for $C_{20}H_{27}N_3O_6S$: C, 54.90; H, 6.22; N, 9.60. Found: C, 54.73; H, 6.18; N, 9.61. $[\alpha]_D^{25}$ −22.4 (c 1.10, MeOH).

(R)-N-(1-(3-(Cyclopropylmethoxy)-4-fluorophenyl)ethyl)-3-((2,4-dioxo-3,4-dihydropyrimidin-1(2H)-yl)methoxy)propane-1-sulfonamide (26). 26 was prepared from 28 (145 mg, 0.39 mmol) as described for the preparation of 16; colorless gum (54.9 mg, 0.12 mmol, 31%). ^{1}H NMR (270 MHz, CDCl$_3$) δ 0.31−0.38 (2H, m), 0.59−0.69 (2H, m), 1.20−1.38 (1H, m), 1.52 (3H, d, J = 6.8 Hz), 1.80−1.98 (2H, m), 2.51−2.88 (2H, m), 3.53 (2H, t, J = 5.9 Hz), 3.88 (2H, d, J = 7.0 Hz), 4.57 (1H, quin, J = 6.8 Hz), 4.72 (1H, brs), 5.06 (2H, s), 5.77 (1H, dd, J = 8.1 Hz, 1.6 Hz), 6.85−7.11 (3H, m), 7.24−7.27 (1H, m), 8.53 (1H, brs). ^{13}C NMR (100 Mz, CDCl$_3$) δ 3.3, 10.2, 23.7, 24.0, 50.3, 53.2, 66.9, 74.4, 76.5, 103.2, 113.7 (d, J = 6.6 Hz), 116.3 (dd, J = 19.0, 5.0 Hz), 118.7 (t, J = 4.1 Hz), 139.1, 143.3 (d, J = 11.6 Hz), 147.1 (d, J = 10.8 Hz), 151.1, 152.1 (d, J = 246.5 Hz), 163.6. Anal. Calcd for $C_{20}H_{26}FN_3O_6S$: C, 52.74; H, 5.75; N, 9.23. Found: C, 52.56; H, 5.48; N, 9.23. $[\alpha]_D^{25}$ + 13.9 (c 1.00, CHCl$_3$).

Cloning, Expression and Purification of Recombinant Human dUTPase. The cDNA of human dUTPase was subcloned into the expression vector pET19b. The construct was then transformed into *E. coli* BL21(DE3) cells (Novagen) in Luria broth at 37 °C. Protein expression was induced with 0.01 mM isopropyl-β-D-thiogalactopyranoside (IPTG) at an optical density of 0.6 at 595 nm. The cell pellet was resuspended in ice-cold lysis buffer containing 50 mM Tris-HCl pH 7.5, 150 mM NaCl, and 1 mM dithiothreitol (DTT). After sonication, the disrupted debris was removed by centrifugation. The supernatant was applied to Ni-NTA affinity gels, and the 6 × His-Tag was removed by digestion with enterokinase in 50 mM Tris-HCl pH 7.5, 150 mM NaCl, and 1 mM DTT for 12 h. The protein solutions used for crystallization were gelfiltrated in a buffer containing 50 mM Tris-HCl pH 7.5, 50 mM NaCl, and 1 mM DTT on a preparative grade Superdex 75 column (GE Healthcare Life Sciences).

Crystallization and Data Collection. The protein solution prepared for cocrystallization contained 20 mg/mL dUTPase, 0.1 mM compound 9, and 10 mM MgCl$_2$. Crystallization experiments were carried out by the hanging-drop vapor diffusion method. Crystals were obtained at 25 °C from the reservoir solution consisting of 15%−20% PEG 4000, 50 mM Tris-HCl pH 7.5, 15% (v/v) glycerol, and 50 mM MgCl$_2$. X-ray data were collected from a cryo-cooled (100 K) crystal at Pharmaceutical Industry Beamline (BL32B2) (Harima, Japan) using a RAXIS V (Rigaku Corporation) imaging plate (IP) area

detector. The data, extending to 1.8 Å (3ARN), were integrated and scaled using the CrystalClear software package (Rigaku Corporation).

Structure Determination and Refinement. The structure of dUTPase complexed with compound 9 was solved by molecular replacement using the program AMoRe[37] from the CCP4 suite.[38] The search model was based on human dUTPase structure (PDB ID: 1Q5U). The structure of dUTPase complexed to compound 9 was refined using REFMAC5.[39] Manual rebuilding of the models and electron density map interpretation were carried out using Turbo-Frodo.[40] The final model has R values of R_{cryst} = 17.2%, R_{free} = 19.7%. A summary of statistics from the data collection and refinement is given in Table 6.

Table 6. X-Ray Crystallography Data and Refinement Statistics

dUTPase with compd 9 (PDB ID: 3ARN)	
Crystal Data	
$P2_12_12_1$ cell dimensions (Å)	a = 82.40, b = 83.15, c = 89.59
resolution range (Å)	60.94−1.80 (1.86−1.80)
no. observed reflections	400353
no. unique reflections	57479
completeness of data (%)	99.6 (99.1)
R_{sym} [a]	0.040 (0.119)
$I/\sigma I$	29.3 (11.8)
Refinement Statistics	
resolution range (Å)	58.53−1.80 (1.85−1.80)
R_{cryst} (no ó cutoff) (%) [b]	17.2 (25.70)
no. reflections in work set	51657 (3946)
R_{free} (no ó cutoff) (%) [c]	19.8 (31.60)
no. reflections in test set	2911 (187)
rmsd bonds (Å) [d]	0.032
rmsd angles (deg) [d]	2.443
no. nonhydrogen atoms	3427
no. protein/inhibiter/water/Mg atoms	2922/78/421/6
average B-factor (Å^2) for all atoms	17.21
average B-factor (Å^2) for protein/inhibitor/water/Mg	16.26/14.65/24.24/25.67

[a] $R_{sym} = \sum \sum_j |I_j - \langle I \rangle| / \sum \langle I \rangle$, where I_j is the recorded intensity of the jth reflection and $\langle I \rangle$ is the average intensity over multiple recordings. [b] $R_{cryst} = \sum_h ||F_o(h)| - |F_c(h)|| / \sum_h |F_o(h)|$, where $F_o(h)$ and $F_c(h)$ are observed and calculated structure factors. [c] R_{free} values are calculated for a randomly selected 5% of the data which were omitted the refinement. [d] Root mean square deviation from ideal/target geometries.

dUTPase Inhibition Assay. In vitro dUTPase inhibition assays were conducted by measuring the production of [5-^{3}H]dUMP from [5-^{3}H]dUTP. Briefly, 0.2 mL of a solution containing 0.02 mL of 1 μM dUTP (including 588 Bq/mL [5-^{3}H]dUTP), 0.05 mL of 0.2 M Tris buffer solution (pH 7.4), 0.05 mL of 16 mM magnesium chloride, 0.02 mL of 20 mM 2-mercaptoethanol, 0.02 mL of a 1% aqueous solution of fetal bovine serum-derived albumin, 0.02 mL of varying concentrations of test compound solutions or pure water as a control, and 0.02 mL of a solution of human dUTPase was reacted at 37 °C for 15 min. After the reaction, the solution was immediately heated at 100 °C for 1 min to terminate the reaction and then centrifuged at 15000 rpm for 2 min. An aliquot (150 μL) of the supernatant thus obtained by centrifugation was analyzed using an Atlantis C18 column (manufactured by Waters Corp., 4.6 mm × 250 mm) and a high-performance liquid chromatograph (manufactured by Shimadzu Corp., Prominence). The inhibition rate of the compound was determined according to the formula shown below. IC$_{50}$ (μM), the concentration

of inhibitor yielding 50% inhibition rate, was obtained from concentration−inhibition rate curve.

$$\begin{aligned} \text{Inhibitory rate(\%)} = 1 - & \left[(\text{amount of} [5\text{-}^3\text{H}] \right. \\ & \text{dUMP in presence of test solution(dpm))} \\ & \left. /(\text{amount of} [5\text{-}^3\text{H}]\text{dUMP as control(dpm)}) \right] \times 100 \end{aligned}$$

In Vitro Cell Inhibition Assays. HeLa S3 (human cervix adenocarcinoma) cells were cultured in RPMI1640 supplemented with 10% FBS. Exponentially growing cells were seeded in 96-well plates (1500 cells/0.18 mL) and incubated at 37 °C in a humidified 5% CO_2 atmosphere for 24 h. Vehicle-control (DMSO) and test compounds (1−100 μM) were added to the plates at a volume of 20 μL per well, and the plates were incubated for 72 h. Cell proliferation was determined by the Crystal Violet assay. Optical density at 540 nm (OD_{540}) was measured by plate reader. Then, we calculated T/C (%) value, which was the ratio of OD_{540} with drug treatment to without drug {T/C (%) = (OD_{540} of treated well/OD_{540} of nontreated well) × 100}. The IC_{50} (μM) for the cytotoxicity of the test compound was the concentration yielding 50% T/C value, which was calculated from concentration−T/C (%) curve.

In Vitro Cell Inhibition Assays in Combination with FdUrd. HeLa S3 cells were seeded in 96-well plates (1500 cells/0.18 mL) and incubated at 37 °C in a humidified 5% CO_2 atmosphere as described above. After 24 h, vehicle-control (DMSO) and test compounds (1−100 μM) in combination with FdUrd (1 μM) were added to the plates at a volume of 20 μL per well and incubated for 24 h. Then, thymidine (30 μM) was added to the plates at a volume of 10 μL per well and incubated for 48 h. Cell proliferation was determined by the Crystal Violet assay as mentioned above. The EC_{50} value was calculated from the concentration−T/C (%) curve as a concentration of each compound that reduces the T/C (%) value of FdUrd (1 μM) against HeLa S3 cells to half in 24 h.

Pharmacokinetic Studies. Experiments were conducted with 6-week-old to 9-week-old male Balb/c-A mice. Compound **26** was administered to mice orally at a dose of 50 mg/kg in a solution containing 2.5% DMA, 2.5% Tween 80, and 10% Cremophor EL. The concentration of **26** in the plasma was determined by ultraperformance liquid chromatography (UPLC).

Evaluation of Antitumor Efficacy of Compound 26. Five-week-old Balb/cA JcL-nu mice were obtained from Clea Japan, Inc. (Tokyo, Japan). MX-1 human breast carcinoma (Japanese Foundation For Cancer Research) was maintained by subcutaneous (sc) transplantation in mice. Briefly, tumors were excised, and fragments (approximately 2 mm in diameter) were implanted sc using a trocar. After implantation, the animals were divided into four groups and treated with either vehicle (2.5% DMA, 2.5% Tween 80, 10% Cremophor, and 0.5% HPMC), 5-FU (15 mg/kg/day) by continuous infusion using osmotic pump for 14 days, compound **26** (300 mg/kg/mg) by po for 14 days, or with the combination of 5-FU (15 mg/kg/day) and compound **26** (300 mg/kg/mg). Tumor size and body weight were measured twice weekly. Tumor volume (TV) were estimated with the formula: TV (mm^3) = length (mm) × width (mm) × width (mm) × 0.5. Relative tumor volume (RTV) on day 15 was calculated as the ratio of TV on day 15 to that on day 0 according to the following formula: RTV = [(TV on day 15)/(TV on day 0)]. Body weight change (%) on day 15 was calculated according to the following formula: body weight change (%) = {[(body weight on day 15) − (body weight on day 0)]/(body weight on day 0)} × 100.

ASSOCIATED CONTENT

S **Supporting Information**

Synthetic procedures and characterization data for compounds **8**, **27**, **28**, **29R**, **29S**, and **29R/S**. This material is available free of charge via the Internet at http://pubs.acs.org.

Accession Codes

PDB code of compound **9** with human dUTPase: 3ARN.

AUTHOR INFORMATION

Corresponding Author

*Phone: 81-29-865-4527. Fax: 81-29-865-2170. E-mail: m-fukuoka@taiho.co.jp.

Notes

The authors declare no competing financial interest.

ACKNOWLEDGMENTS

ABBREVIATIONS USED

dUTPase, deoxyuridine triphosphatase; dUTP, 2′-deoxyuridine 5′-triphosphate; dTTP, thymidine 5′-triphosphate; dUMP, 2′-deoxyuridine 5′-monophosphate; TS, thymidylate synthase; 5-FU, 5-fluorouracil; FdUrd, 5-fluoro-2′-deoxyuridine; FdUTP, 5-fluoro-2′-deoxyuridine 5′-triphosphate; SAR, structure−activity relationship; MOM, methoxymethyl

REFERENCES

(1) Longley, D. B.; Harkin, D. P.; Johnston, P. G. 5-Fluorouracil: mechanisms of action and clinical strategies. *Nature Rev. Cancer* **2003**, *3*, 330−338.

(2) Danneberg, P. B.; Montag, B. J.; Heidelberger, C. Studies on fluorinated pyrimidines. IV. Effects on nucleic acid metabolism in vivo. *Cancer Res.* **1958**, *18*, 329−334.

(3) Harrap, K. R.; Jackman, A. L.; Newell, D. R.; Taylor, G. A.; Hughes, L. R.; Calvert, A. H. Thymidylate synthase: a target for anticancer drug design. *Adv. Enzyme Regul.* **1989**, *29*, 161−179.

(4) Jackman, A. L.; Calvert, A. H. Folate-based thymidylate synthase inhibitors as anticancer drugs. *Ann. Oncol.* **1995**, *6*, 871−881.

(5) Popat, S.; Matakidou, A.; Houlston, R. S. Thymidylate synthase expression and prognosis in colorectal cancer: a systematic review and meta-analysis. *J. Clin. Oncol.* **2004**, *22*, 529−536.

(6) Aherne, G. W.; Hardcastle, A.; Raynaud, F.; Jackman, A. L. Immunoreactive dUMP and TTP pools as an index of thymidylate synthase inhibition; effect of tomudex (ZD1694) and a non-polyglutamated quinazoline antifolate (CB30900) in L1210 mouse leukaemia cells. *Biochem. Pharmacol.* **1996**, *51*, 1293−1301.

(7) Mitrovski, B.; Pressacco, J.; Mandelbaum, S.; Erlichman, C. Biochemical effects of folate-based inhibitors of thymidylate synthase in MGH-U1 cells. *Cancer Chemother. Pharmacol.* **1994**, *35*, 109−114.

(8) Cheng, Y. C.; Nakayama, K. Effects of 5-fluoro-2′-deoxyuridine on DNA metabolism in HeLa cells. *Mol. Pharmacol.* **1983**, *23*, 171−174.

(9) Ingraham, H. A.; Tseng, B. Y.; Goulian, M. Nucleotide levels and incorporation of 5-fluorouracil and uracil into DNA of cells treated with 5-fluorodeoxyuridine. *Mol. Pharmacol.* **1982**, *21*, 211−216.

(10) Curtin, N. J.; Harris, A. L.; Aherne, G. W. Mechanism of cell death following thymidylate synthase inhibition: 2′-deoxyuridine-5′-triphosphate accumulation, DNA damage, and growth inhibition following exposure to CB3717 and dipyridamole. *Cancer Res.* **1991**, *51*, 2346−2352.

(11) Webley, S. D.; Hardcastle, A.; Ladner, R. D.; Jackman, A. L.; Aherne, G. W. Deoxyuridine triphosphatase (dUTPase) expression and sensitivity to the thymidylate synthase (TS) inhibitor ZD9331. *Br. J. Cancer* **2000**, *83*, 792−799.

(12) Koehler, S. E.; Ladner, R. D. Small interfering RNA-mediated suppression of dUTPase sensitizes cancer cell lines to thymidylate synthase inhibition. *Mol. Pharmacol.* **2004**, *66*, 620−626.

(13) An, Q.; Robins, P.; Lindahl, T.; Barnes, D. E. 5-Fluorouracil incorporated into DNA is excised by the Smug1 DNA glycosylase to reduce drug cytotoxicity. *Cancer Res.* **2007**, *67*, 940−945.

(14) Shlomai, J.; Kornberg, A. Deoxyuridine triphosphatase of *Escherichia coli* purification, properties, and use as a reagent to reduce uracil incorporation into DNA. *J. Biol. Chem.* **1978**, *253*, 3305−3312.

(15) Bertani, L. E.; Haeggmark, A.; Reichard, P. Enzymatic Synthesis of Deoxyribonucleotides. II. Formation and Interconversion of Deoxyuridine Phosphates. *J. Biol. Chem.* **1963**, *238*, 3407−3413.

(16) Grindey, G. R.; Nichol, C. A. Mammalian deoxyuridine 5′-triphosphate pyrophosphatase. *Biochim. Biophys. Acta* **1971**, *240*, 180−183.

(17) Vertessy, B. G.; Toth, J. Keeping uracil out of DNA: physiological role, structure and catalytic mechanism of dUTPases. *Acc. Chem. Res.* **2009**, *42*, 97−106.

(18) Caradonna, S. J.; Cheng, Y. C. The role of deoxyuridine triphosphate nucleotidohydrolase, uracil−DNA glycosylase, and DNA polymerase alpha in the metabolism of FUdR in human tumor cells. *Mol. Pharmacol.* **1980**, *18*, 513−520.

(19) Canman, C. E.; Lawrence, T. S.; Shewach, D. S.; Tang, H. Y.; Maybaum, J. Resistance to fluorodeoxyuridine-induced DNA damage and cytotoxicity correlates with an elevation of deoxyuridine triphosphatase activity and failure to accumulate deoxyuridine triphosphate. *Cancer Res.* **1993**, *53*, 5219−5224.

(20) Canman, C. E.; Radany, E. H.; Parsels, L. A.; Davis, M. A.; Lawrence, T. S.; Maybaum, J. Induction of resistance to fluorodeoxyuridine cytotoxicity and DNA damage in human tumor cells by expression of *Escherichia coli* deoxyuridinetriphosphatase. *Cancer Res.* **1994**, *54*, 2296−2298.

(21) Wilson, P. M.; Fazzone, W.; LaBonte, M. J.; Deng, J.; Neamati, N.; Ladner, R. D. Novel opportunities for thymidylate metabolism as a therapeutic target. *Mol. Cancer Ther.* **2008**, *7*, 3029−3037.

(22) Ladner, R. D.; Lynch, F. J.; Groshen, S.; Xiong, Y. P.; Sherrod, A.; Caradonna, S. J.; Stoehlmacher, J.; Lenz, H. J. dUTP nucleotidohydrolase isoform expression in normal and neoplastic tissues: association with survival and response to 5-fluorouracil in colorectal cancer. *Cancer Res.* **2000**, *60*, 3493−3503.

(23) Takatori, H.; Yamashita, T.; Honda, M.; Nishino, R.; Arai, K.; Takamura, H.; Ohta, T.; Zen, Y.; Kaneko, S. dUTP pyrophosphatase expression correlates with a poor prognosis in hepatocellular carcinoma. *Liver Int.* **2010**, *30*, 438−446.

(24) Zalud, P.; Wachs, W. O.; Nyman, P. O.; Zeppezauer, M. M. Inhibition of the proliferation of human cancer cells in vitro by substrate-analogous inhibitors of dUTPase. *Adv. Exp. Med. Biol.* **1994**, *370*, 135−138.

(25) Persson, T.; Larsson, G.; Nyman, P. O. Synthesis of 2′-deoxyuridine 5′-(alpha,beta-imido) triphosphate: a substrate analogue and potent inhibitor of dUTPase. *Bioorg. Med. Chem.* **1996**, *4*, 553−556.

(26) Barabas, O.; Pongracz, V.; Kovari, J.; Wilmanns, M.; Vertessy, B. G. Structural insights into the catalytic mechanism of phosphate ester hydrolysis by dUTPase. *J. Biol. Chem.* **2004**, *279*, 42907−42915.

(27) Pecsi, I.; Leveles, I.; Harmat, V.; Vertessy, B. G.; Toth, J. Aromatic stacking between nucleobase and enzyme promotes phosphate ester hydrolysis in dUTPase. *Nucleic Acids Res.* **2010**, *38*, 7179−7186.

(28) Kovari, J.; Barabas, O.; Varga, B.; Bekesi, A.; Tolgyesi, F.; Fidy, J.; Nagy, J.; Vertessy, B. G. Methylene substitution at the alpha-beta bridging position within the phosphate chain of dUDP profoundly perturbs ligand accommodation into the dUTPase active site. *Proteins* **2008**, *71*, 308−319.

(29) Nguyen, C.; Kasinathan, G.; Leal-Cortijo, I.; Musso-Buendia, A.; Kaiser, M.; Brun, R.; Ruiz-Perez, L. M.; Johansson, N. G.; Gonzalez-Pacanowska, D.; Gilbert, I. H. Deoxyuridine triphosphate nucleotidohydrolase as a potential antiparasitic drug target. *J. Med. Chem.* **2005**, *48*, 5942−5954.

(30) Whittingham, J. L.; Leal, I.; Nguyen, C.; Kasinathan, G.; Bell, E.; Jones, A. F.; Berry, C.; Benito, A.; Turkenburg, J. P.; Dodson, E. J.; Ruiz Perez, L. M.; Wilkinson, A. J.; Johansson, N. G.; Brun, R.; Gilbert, I. H.; Gonzalez Pacanowska, D.; Wilson, K. S. dUTPase as a platform for antimalarial drug design: structural basis for the selectivity of a class of nucleoside inhibitors. *Structure* **2005**, *13*, 329−338.

(31) Nguyen, C.; Ruda, G. F.; Schipani, A.; Kasinathan, G.; Leal, I.; Musso-Buendia, A.; Kaiser, M.; Brun, R.; Ruiz-Perez, L. M.; Sahlberg, B. L.; Johansson, N. G.; Gonzalez-Pacanowska, D.; Gilbert, I. H. Acyclic nucleoside analogues as inhibitors of *Plasmodium falciparum* dUTPase. *J. Med. Chem.* **2006**, *49*, 4183−4195.

(32) Hampton, S. E.; Baragana, B.; Schipani, A.; Bosch-Navarrete, C.; Musso-Buendia, J. A.; Recio, E.; Kaiser, M.; Whittingham, J. L.; Roberts, S. M.; Shevtsov, M.; Brannigan, J. A.; Kahnberg, P.; Brun, R.; Wilson, K. S.; Gonzalez-Pacanowska, D.; Johansson, N. G.; Gilbert, I. H. Design, synthesis, and evaluation of 5′-diphenyl nucleoside analogues as inhibitors of the *Plasmodium falciparum* dUTPase. *ChemMedChem* **2011**, *6*, 1816−1831.

(33) Jiang, Y. L.; Chung, S.; Krosky, D. J.; Stivers, J. T. Synthesis and high-throughput evaluation of triskelion uracil libraries for inhibition of human dUTPase and UNG2. *Bioorg. Med. Chem.* **2006**, *14*, 5666−5672.

(34) Miyakoshi, H.; Miyahara, S.; Yokogawa, T.; Chong, K. T.; Taguchi, J.; Endoh, K.; Yano, W.; Wakasa, T.; Ueno, H.; Takao, Y.; Nomura, M.; Shuto, S.; Nagasawa, H.; Fukuoka, M. Synthesis and discovery of *N*-carbonylpyrrolidine- or *N*-sulfonylpyrrolidine-containing uracil derivatives as potent human dUTPase inhibitors. *J. Med. Chem.* 10.1021/jm201101627n.

(35) Mol, C. D.; Harris, J. M.; McIntosh, E. M.; Tainer, J. A. Human dUTP pyrophosphatase: uracil recognition by a beta hairpin and active sites formed by three separate subunits. *Structure* **1996**, *4*, 1077−1092.

(36) Varga, B.; Barabas, O.; Kovari, J.; Toth, J.; Hunyadi-Gulyas, E.; Klement, E.; Medzihradszky, K. F.; Tolgyesi, F.; Fidy, J.; Vertessy, B. G. Active site closure facilitates juxtaposition of reactant atoms for initiation of catalysis by human dUTPase. *FEBS Lett.* **2007**, *581*, 4783−4788.

(37) Navaza, J. AMoRe: an automated package for molecular replacement. *Acta Crystallogr., Sect. A: Found. Crystallogr.* **1994**, *A50*, 157−163.

(38) Collaborative Computational Project No. 4. The CCP4 suite: programs for protein crystallography. *Acta Crystallogr., Sect. D: Biol. Crystallogr.* **1994**, *D50*, 760−763.

(39) Murshudov, G. N.; Vagin, A. A.; Dodson, E. J. Refinement of macromolecular structures by the maximum-likelihood method. *Acta Crystallogr., Sect. D. Biol. Crystallogr.* **1997**, *D53*, 240−255.

(40) Roussel, A.; Cambillau, C. TURBO-FRODO Molecular Graphics Profram. In *Silicon Graphics Geometry Partner Directory*; Silicon Graphics: Mountain View, CA, 1989; pp 77−78.